

NO_x Emission Reduction by Advanced Reburning in Grate-Rotary Kiln for the Iron Ore Pelletizing Production

Authors:

Bing Hu, Peiwei Hu, Biao Lu, Zhicheng Xie, Liu Liu, Gangli Cheng, Jiaoyang Wei

Date Submitted: 2021-05-27

Keywords: NO_x reduction, grate-rotary kiln, denitrification, advanced reburning

Abstract:

The NO_x reduction in the iron ore pelletizing process becomes an important environmental concern owing to its role in the formation of photochemical smog and acid rain. Thus, it is essential to develop new technologies for reducing NO_x emissions in order to contribute to the cleaner production of pellets. In this paper, NO_x reduction by advanced reburning in grate-rotary kiln for oxidized pellet production was performed on a laboratory-scale gas kiln. Temperature and NH₃/NO_x molar ratio (NSR) were the key factors affecting the reduction of NO_x. A better denitrification effect can be obtained on flue gas with higher initial NO_x concentration, at temperature = 900 °C, NSR = 1.2, and reaction time exceeds one second. NO_x reduction rate had reached 55-65% when the initial NO_x concentration was above 400 ppm, and exceeds 70% when the initial NO_x concentration was around 680 ppm. Urea solution has the best denitrification effect compared with NH₃-H₂O and NH₄HCO₃ solution. As for additives, the denitrification effect of the vanadium-titanium catalyst was better than that of ethanol and NaCl, while NaCl plays a promotive role at low NSR. Finally, a series of denitrification measures that include advanced reburning technology for achieving NO_x ultra-low emission in the oxidation pellet production was proposed.

Record Type: Published Article

Submitted To: LAPSE (Living Archive for Process Systems Engineering)

Citation (overall record, always the latest version):

LAPSE:2021.0471

Citation (this specific file, latest version):

LAPSE:2021.0471-1

Citation (this specific file, this version):


LAPSE:2021.0471-1v1

DOI of Published Version: <https://doi.org/10.3390/pr8111470>

License: Creative Commons Attribution 4.0 International (CC BY 4.0)

Article

NO_x Emission Reduction by Advanced Reburning in Grate-Rotary Kiln for the Iron Ore Pelletizing Production

Bing Hu ¹, Peiwei Hu ^{2,3,*}, Biao Lu ⁴, Zhicheng Xie ², Liu Liu ² , Gangli Cheng ² and Jiaoyang Wei ²

¹ National Engineering Research Center of Sintering and Pelletizing Equipment System, Zhongye Changtian International Engineering Co., Ltd., Changsha 410205, China; csu0206@163.com

² College of Resources and Environment Engineering, Wuhan University of Science and Technology, Wuhan 430081, China; xzc2021@163.com (Z.X.); liuliuwust@163.com (L.L.); glclucky@163.com (G.C.); streamwjy@163.com (J.W.)

³ Hubei Key Laboratory for Efficient Utilization and Agglomeration of Metallurgic Mineral Resources, Wuhan University of Science and Technology, Wuhan 430081, China

⁴ School of Minerals Processing & Bioengineering, Central South University, Changsha 410083, China; lubiao0815@hotmail.com

* Correspondence: pwhu@wust.edu.cn; Tel.: +86-27-6886-2204

Received: 19 October 2020; Accepted: 10 November 2020; Published: 16 November 2020



Abstract: The NO_x reduction in the iron ore pelletizing process becomes an important environmental concern owing to its role in the formation of photochemical smog and acid rain. Thus, it is essential to develop new technologies for reducing NO_x emissions in order to contribute to the cleaner production of pellets. In this paper, NO_x reduction by advanced reburning in grate-rotary kiln for oxidized pellet production was performed on a laboratory-scale gas kiln. Temperature and NH₃/NO_x molar ratio (NSR) were the key factors affecting the reduction of NO_x. A better denitrification effect can be obtained on flue gas with higher initial NO_x concentration, at temperature = 900 °C, NSR = 1.2, and reaction time exceeds one second. NO_x reduction rate had reached 55–65% when the initial NO_x concentration was above 400 ppm, and exceeds 70% when the initial NO_x concentration was around 680 ppm. Urea solution has the best denitrification effect compared with NH₃·H₂O and NH₄HCO₃ solution. As for additives, the denitrification effect of the vanadium-titanium catalyst was better than that of ethanol and NaCl, while NaCl plays a promotive role at low NSR. Finally, a series of denitrification measures that include advanced reburning technology for achieving NO_x ultra-low emission in the oxidation pellet production was proposed.

Keywords: advanced reburning; denitrification; grate-rotary kiln; NO_x reduction

1. Introduction

Iron ore pellets are a main iron-bearing burden for the blast furnace ironmaking process [1,2]. Because of its good metallurgical properties and low energy consumption in the production process, pellets can increase production, save coke, improve technical and economic indexes of ironmaking, reduce hot metal cost and improve economic benefits when applied to the blast furnace ironmaking process, as a consequence, it has been developed rapidly. The world's pellet production was close to 450 million tons in 2015, and China's annual pellet production peaked 200 million tons in 2011 [3–7]. However, with the increasingly strict environmental protection requirements, China has formulated a series of emission standards for iron and steel enterprises, forcing pelletizing plants to do corresponding work in environmental protection. Although dust removal and desulfurization can meet

the emission targets, NO_x emission has become a restriction factor in the development and production of pelletizing plants because of its high removal cost and complex process [8–10]. Pellet production in China is mainly produced by a grate-rotary kiln process, and its output accounts for nearly 60% of the output of the total pellet [11,12]. Many studies have shown that NO_x formation in rotary kilns occurs in the flame, due to either the high temperatures (thermal NO_x) or the oxidation of the fuel-bound nitrogen [13,14]. When coal is combusted in iron-ore rotary kilns, the NO_x formation is dominated by the conversion of char-N to NO [15,16]. At present, NO_x emission reduction is mainly accomplished through reducing the injection of coal gas or pulverized coal, reducing rotary kiln temperature, and using lower NO_x raw materials and fuels in China's pelletizing plants. Although these measures can reduce the emission of NO_x to a certain extent, it will cause the decline of pellet output and quality, which goes against the normal production and development of pelletizing plants. Besides, the reason for the low efficiency of primary measures is that most focus on suppressing the formation of NO_x from the volatile nitrogen or the thermal NO mechanism. For the purpose of the desired reduction in NO_x formation, a recent study by Edland, R. et al. suggested that more drastic measures must be implemented, such as switching fuel or designing the process so that the excess air can be reduced. Their simulations showed that replacing the reference coal with a biomass that contains 0.1% nitrogen can reduce NO_x emissions by 90% [17]. Generally, the emission concentration of nitrogen oxides from pelletizing plants are generally between 150 mg/m^3 and 300 mg/m^3 , which causes great pollution to the environment and is far from meeting the requirements of today's environmental protection; hence, it is urgent for modern iron and steel enterprises to develop novel NO_x reduction approaches in the grate-rotary kiln process.

Nitrogen oxides (NO_x , $x = 1,2$), as major air pollutants, are resulting in a series of environmental issues, such as photochemical smog, acid rain, ozone depletion, and fine particle pollution. Many efforts have been made to reduce NO_x emission by using advanced combustion technologies or by using post-combustion abatement technologies [18,19]. Among various kinds of NO_x removal technologies, a simple process for reducing NO_x to nitrogen and water is an ideal way. Two major post-combustion NO_x control techniques are selective catalytic reduction and selective non-catalytic reduction, which are widely used in large combustion units, such as various boilers, refineries, and waste incinerators [20–22]. There have been many investigations on the effect of parameters on the performance of NO_x catalytic reduction in the laboratory, but several investigations have been reported about NO_x reduction by advanced reburning, the effects of temperature, NH_3/NO_x molar ratio (NSR), and other factors on NO_x reduction have been studied, under the optimized conditions, the efficiency NO_x reduction of advanced reburning could potentially increase to more than 85% [23–27]. However, these investigations are mainly focused on cement precalciner kilns and utility boilers; the application of advanced reburning in oxidized pellet production has not been reported yet. Besides, many experiments were performed in various laboratory-scale reactor, all of them which temperature was controlled by an electric heating furnace, designed to maintain the reaction temperature at the desired value, and the NO_x reduction reaction process in a gas-fired environment does not simulate well. Thus, the advanced reburning of in grate-rotary kiln needs further study.

The objective of this present study was to investigate the influences of temperature, NSR, and other factors on NO_x reduction and ammonia slip, by advanced reburning; as well as to optimize the operating parameters of the grate-rotary kiln for the better development of pellet production, and then proposes the mechanism or the most rational operating technology that contribute to a further reduction in the NO_x content of exhaust gas in the iron ore pelletizing production.

2. Materials and Methods

The chemicals used in the laboratory-scale gas kiln test, including the ammonia liquor ($\text{NH}_3 \cdot \text{H}_2\text{O}$), ammonium bicarbonate (NH_4HCO_3), urea ($\text{CH}_4\text{N}_2\text{O}$), sodium chloride (NaCl), ethanol absolute ($\text{C}_2\text{H}_6\text{O}$), were analytically pure and used without further treatment. Vanadium-titanium catalyst, obtained from national engineering laboratory for multi-flue gas pollution control technology and

equipment of China, was milled to produce ultrafine powders. NO (purity $\geq 99.9\%$) used in this work was purchased from Wuhan new radar special gas co., ltd. In the Hubei province of China.

In this paper, the advanced reburning in a grate-rotary kiln for NO_x reduction was performed on a laboratory-scale gas kiln. The experimental system schematic is shown in Figure 1a, and a photograph of the grate-rotary kiln in Figure 1b–d. The inner diameter of the gas kiln is 0.4 m, and its length is 5 m. A gas burner was equipped at the head of the kiln, and an auxiliary heating device was installed on the middle side. Gas and air were pumped into the burner for combustion, and the temperature was regulated by gas flowmeters. Four temperature measuring points were arranged in the kiln body by inserting thermocouples.

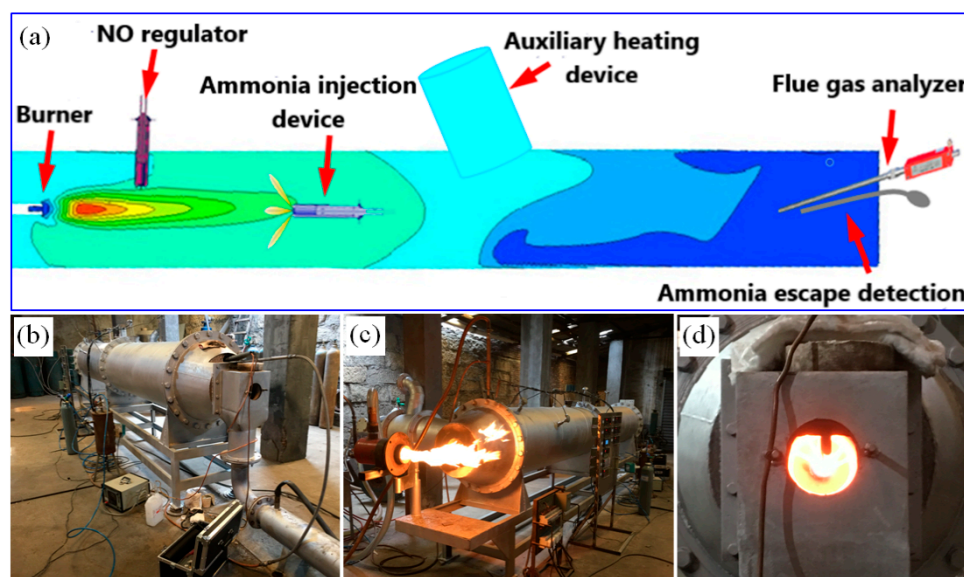


Figure 1. Schematic of the experimental system (a) and the laboratory-scale gas kiln (b–d).

NO was injected into the front side of the kiln, and the gas concentration was controlled by a gas flowmeter. NH₃·H₂O injection device was inserted from the tail of the kiln, and the insertion length can be adjusted, and the amount of NH₃·H₂O injection was regulated by a liquid flowmeter. In addition, flue gas analyzer and ammonia slip detection device were also inserted from the tail of kiln. The experimental conditions of each group lasted for more than 6 min. The data were recorded every 2 min, and the average value was taken as the experimental results. The composition of flue gas was measured by German MRU Nova plus multi-functional flue gas analyzer through the probe, mainly including the concentration of O₂, CO₂, CO, NO, and NO_x. The concentration of O₂ and CO₂ were expressed as a percentage, and the concentration of CO, NO, and NO_x as a ppm. The monitoring point in the rotary kiln, as shown in Figure 1. The NO_x reduction efficiency was calculated by the following Formula (1):

$$\eta_{NO_x} = (C_{NO_x,in} - C_{NO_x,out})/C_{NO_x,in} \times 100\% \quad (1)$$

where η_{NO_x} was the NO_x reduction rate (%), $C_{NO_x,in}$ (ppm) and $C_{NO_x,out}$ (ppm) were the inlet and outlet concentrations of NO_x, respectively.

The determination of ammonia concentration in flue gas was referred to as the National Environmental Protection Standard of China “Determination of Ammonia in Ambient Air and Exhaust Gas by Nessler Reagent Spectrophotometer” (HJ 533-2009). The schematic diagram of the determination for ammonia slip, as shown in Figure 2. The principle as follows: The ammonia in flue gas was absorbed by dilute sulfuric acid firstly, and then the generated ammonium ion reacts with Nessler’s reagent to a form yellow-brown complex. The absorbance of the sampling absorption solution was measured at a wavelength of 420 nm. Since the absorbance of the above complex was

proportional to the content of ammonia in solution, the ammonia content in the gas can be calculated based on the absorbance.

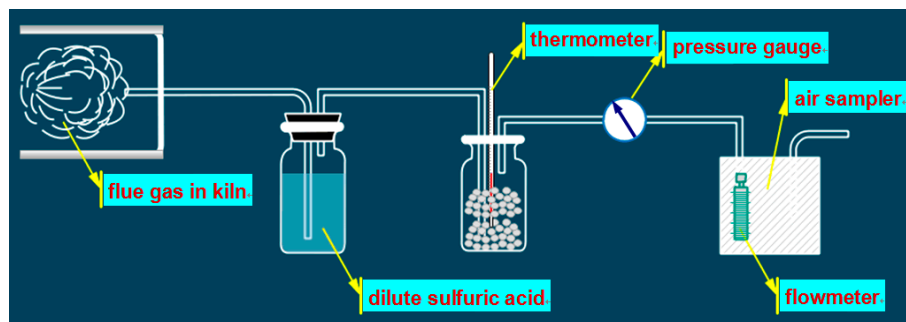


Figure 2. Schematic diagram of the determination for ammonia slip.

The ammonia concentration in flue gas (ρ_{NH_3}) was obtained using the following Formula (2):

$$\rho_{NH_3} = (A - A_0 - a) \times V_s \times D / (b \times V_{nd} \times V_0) \quad (2)$$

where ρ_{NH_3} is the ammonia slip concentration (mg/m^3), A is the absorbance of sample absorption solution, A_0 is the absorbance of the blank absorption solution prepared in the same batch, a is the intercept of the calibration curve, b is the slope of the calibration curve, V_s is the volume of sample absorption solution (mL), V_0 is the volume of absorption liquid taken during analysis (mL), V_{nd} is the standard volume (101.325 kPa, 273 K) of the flue gas (L), and D is Dilution factor.

The standard volume of the flue gas (V_{nd}) was calculated by the following Formula (3):

$$V_{nd} = V \times P \times 273 / [101.325 \times (273 + t)] \quad (3)$$

where V is the sampling volume (L), P is the atmospheric pressure during sampling, and t is the flue gas temperature during sampling.

3. Results and Discussion

3.1. Effect of Reaction Parameters on the NO_x Reduction

Figure 3a showed the effects of temperature on the NO_x reduction and ammonia slip when the NSR was around 1.1, and the initial concentration of NO_x was about 390 ppm. It can be seen that excessive temperature was not conducive to reducing NO_x , the NO_x reduction rate slightly increased first and then decreased sharply with the rise of temperature, and the NO_x reduction rate reached the highest of 71.3% at 890 °C.

Temperature determines the reaction rate of the following two reactions:



when the temperature is lower than the appropriate temperature for the above reactions, the generation of OH and O is limited, which makes it difficult for reactions (6) and (7) to proceed and cannot produce enough NH_2 with high selectivity for NO reduction.



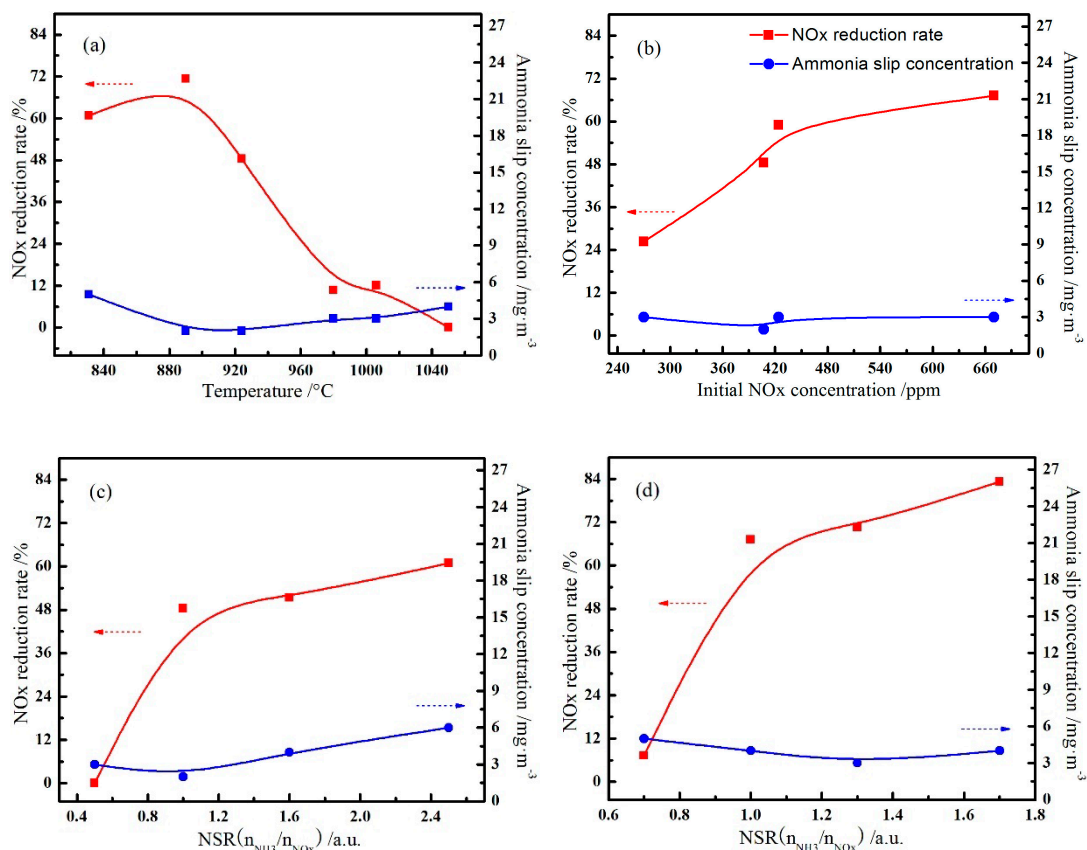
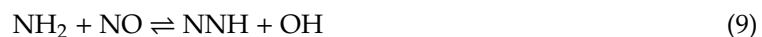


Figure 3. Effects of reaction conditions on the NO_x reduction. (Reaction temperature (a); initial NO_x concentration (b); the [NH₃/NO_x] molar ratio with the initial NO_x concentration was 390 ppm (c) and 680 ppm (d)).

As the temperature rises to a suitable range, reactions (4) and (5) proceed rapidly, resulting in a large number of OH and O. With its increase, a large number of NH₃ is converted into NH₂, which triggers the whole chain reaction, and NO is rapidly reduced as reactions (8)–(10). However, when the temperature continues to rise, the OH produced by reactions (4) and (5) continues to accumulate, and excessive OH will continue to dehydrogenate NH₂ to form NH, as reaction (11) shows, which will be oxidized to NO by oxygen at high temperature through reactions (12)–(15), resulting in a decrease in the NO reduction rate [28,29].



The same rule can be obtained by increasing the NSR, it was unfavorable to NO_x reduction when the temperature goes above 1000 °C, as NO_x reduction rate decreased from 66.3% to 48.0% when the temperature increased from 946 °C to 1010 °C under the condition of NSR = 2.0. Besides, excessive and low temperature will both cause increase of ammonia slip concentration, which also hit a minimum

of 2 mg/m^3 at $890 \text{ }^\circ\text{C}$ and $\text{NSR} = 1.1$, but overall the higher NSR value results in more ammonia slip, as the ammonia slip concentration was greater than or equal to 5 mg/m^3 at $\text{NSR} = 2.0$.

Figure 3b showed the effects of initial NO_x concentration on the NO_x reduction and ammonia slip when the NSR was around 1.1 and the temperature at about $920 \text{ }^\circ\text{C}$. Obviously, NO_x reduction rate has a certain relationship with the initial NO_x concentration, it showed that with the increase of initial NO_x concentration, NO_x reduction rate increased gradually, while the ammonia slip did not change much. Under the suitable NSR, the reaction rate of reactions (8)–(10) increased when the initial concentration of NO_x increases, so NO_x reduction rate is also increased. But at this point, the initial concentration of NO_x is not the limiting factor of the whole denitrification reaction, so the increase of NO_x reduction rate is not obvious. As shown in Figure 3b, it was more appropriate to complete denitrification in an atmosphere with a higher initial NO_x concentration, as a consequence, grate PH zone is a suitable place to install denitrification devices in grate-rotary kiln process for its high NO_x concentration.

Figure 3 also compared the effects of NSR on the NO_x reduction and ammonia slip at different initial NO_x concentrations near $910 \text{ }^\circ\text{C}$. As shown in Figure 3c, when the initial NO_x concentration of flue gas was about 390 ppm, the NO_x reduction rate increased with the increase of $\text{NH}_3\cdot\text{H}_2\text{O}$ consumption, and it reached 48.4% at $\text{NSR} = 1.0$; meanwhile, the ammonia slip concentration was 2 mg/m^3 . Continuously increasing the $\text{NH}_3\cdot\text{H}_2\text{O}$ dosage, the NO_x reduction rate does not change much, but the ammonia slip increases. When NSR increases, the content of NH_3 will also increase, which promotes the reactions (6) and (7) and produces more NH_2 ; thus, more NO will be reduced. When NSR is at a low level, NH_3 becomes the limiting factor of denitrification reaction, therefore, increasing NSR at this time will accelerate reducing NO rapidly. Furthermore, when NSR reaches a certain level, OH will become the limiting link of denitrification reaction, a continuous increase of NSR will not have a significant impact on the NO_x reduction rate.

It can be seen from the Figure 3d that NSR had similar rules on the NO_x reduction rate and ammonia slip when the initial concentration of NO_x rises to 680 ppm, NO_x reduction rate firstly increased sharply as NSR increases, reaching 67.2% with an ammonia slip concentration of 4 mg/m^3 at $\text{NSR} = 1.0$, then it goes through a gentle rise and finally reached 83.3% with an ammonia slip concentration of 4 mg/m^3 at $\text{NSR} = 1.7$. Under the situation of other conditions being equal, it shows better denitrification effect on flue gas with higher initial NO_x concentration, and NSR is one of the main factors affecting the NO_x reduction rate.

3.2. Effects of Reductants on the NO_x Reduction

Table 1 showed the effects of NSR on the NO_x reduction rate and ammonia slip by using 20 wt% NH_4HCO_3 solution as NO_x reducing agent. The results showed that the NH_4HCO_3 solution had little denitrification effect when it was used at low NSR, and NO_x concentration in flue gas even increased slightly at $\text{NSR} = 0.5$. A higher NO_x reduction rate can be obtained by increasing the NSR, and it reached 65.1% at $\text{NSR} = 1.5$, with an ammonia slip concentration of 5 mg/m^3 . But overall, the denitrification effect of NH_4HCO_3 solution was not as good as $\text{NH}_3\cdot\text{H}_2\text{O}$.

Table 1. Effects of reductants on the NO_x reduction with different NH_3/NO_x molar ratio.

NSR	Temperature / $^\circ\text{C}$	Pre-Flue Gas/ppm		Post-Flue Gas/ppm		NO_x Reduction Rate	Ammonia Slip Concentration/ mg m^{-3}	Reductants
		O_2	NO_x	O_2	NO_x			
0.5	933	7.6	519	8.7	525	-	<3.0	NH_4HCO_3 solution
1.0	911	7.6	519	9.0	253	51.3%	<3.0	
1.5	960	7.6	519	8.8	181	65.1%	<5.0	
0.9	923	7.6	457	8.9	174	66.5%	<3.0	urea solution
2.0	933	7.6	457	9.4	142	72.6%	<6.0	

Urea solution, nevertheless, has a better denitrification effect than $\text{NH}_3\cdot\text{H}_2\text{O}$. As shown in Table 1, NO_x reduction rate can reach 66.5% with an ammonia slip concentration of 3 mg/m^3 at $\text{NSR} = 0.9$ when

20 wt% urea solution was used as NO_x reducing agent, and when NSR increased to 2.0, NO_x reduction rate only rises to 72.6%, while ammonia slip concentration reached 6 mg/m³.

3.3. Effects of Additives on the NO_x Reduction

Table 2 compared the effects of three different additives on NO_x reduction and ammonia slip, and the three additives were NaCl, ethanol, and vanadium-titanium catalyst, respectively. Table 2 showed the results of adding 0.1 wt% NaCl to 13 vol.% NH₃·H₂O, it can be seen that the addition of NaCl had a certain effect at low NSR, NO_x reduction rate reached 58.9%, and the ammonia slip concentration was merely 2.0 mg/m³ at NSR = 1.0. However, continuously increased in NSR does not cause significant changes in the NO_x reduction rate, but leads to more ammonia slip.

Table 2. Effects of additives on the NO_x reduction with different NSR.

NSR	Temperature /°C	Pre-Flue Gas/ppm		Post-Flue Gas/ppm		NO _x Reduction Rate	Ammonia Slip Concentration/mg m ⁻³	Additives
		O ₂	NO _x	O ₂	NO _x			
1.0	913	7.8	421	8.3	173	58.9%	<2.0	NaCl
2.0	903	7.8	421	8.8	167	60.3%	<5.0	
2.5	900	7.8	421	9.1	155	63.2%	<7.0	
0.9	927	7.8	421	8.6	300	28.7%	<3.0	ethanol
1.7	912	7.8	421	8.6	136	67.7%	<4.0	
2.5	960	7.8	421	8.5	168	60.1%	<5.0	
1.0	930	8.7	544	9.5	228	58.1%	<3.0	vanadium-titanium catalyst
1.4	928	8.7	544	9.9	177	67.5%	<4.0	
2.5	922	8.7	544	9.7	144	73.5%	<7.0	

Table 2 also showed the effects of NSR on NO_x reduction and ammonia slip when 0.1 vol% ethanol was added to 13 vol.% NH₃·H₂O. Contrary to NaCl, ethanol turns out to be more effective in denitrification at higher NSR, and the NO_x reduction rate reached 67.7% with an ammonia slip concentration of 4.0 mg/m³ at NSR = 1.7. Compared with NaCl and ethanol, the vanadium-titanium catalyst obviously had a better denitrification effect of the overall level. NO_x reduction rate reached 67.5% and the ammonia slip concentration was 4.0 mg/m³ at NSR = 1.4 after 0.05 wt% vanadium-titanium catalyst was added to 13 vol.% NH₃·H₂O. Although a better denitrification effect can be obtained with less dosage of vanadium-titanium catalyst, the cost of vanadium-titanium catalyst is higher than that of the other two additives. Therefore, suitable additives can be selected according to different needs.

3.4. Effects of Process Conditions on the NO_x Reduction

Table 3 showed the effects of O₂ concentration on NO_x reduction and ammonia slip as the NSR was around 1.1, the temperature was near 910 °C, and the initial concentration of NO_x was about 420 ppm. The NO_x reduction rate and ammonia slip did not change much as the O₂ concentration in flue gas varies from 3.8% to 11.2%. NO_x reduction rate only got about 10% promotion, reaching 70.8%, when O₂ concentration increased from 9.0% to 11.2%, while it remains almost unchanged when O₂ concentration increased from 3.8% to 9.0%. Therefore, O₂ concentration had little effect on denitrification efficiency. However, reaction time has a notable influence on the NO_x reduction rate and ammonia slip, and it is detrimental to reducing NO_x when reaction time cannot meet the requirement; at the same time, ammonia slip increases as well. Only when the reaction time is designed to exceed one second can reducing NO_x be guaranteed enough time for its full reaction, achieving a good denitrification effect. Coincidentally, the length of the grate PH zone is usually greater than 10 m, providing sufficient reaction time for NO_x reduction.

Table 3. Effects of process conditions on the NO_x reduction.

NSR	Temperature /°C	Pre-Flue Gas/ppm		Post-Flue Gas/ppm		NO _x Reduction Rate	Ammonia Slip Concentration/mg m ⁻³	Process Conditions	
		O ₂	NO _x	O ₂	NO _x				
1.0	901	11.2	415	11.2	121	70.8%	<2.0	11.2	
1.1	918	9.0	424	9.3	174	59.0%	<3.0	9.0	O ₂ /%
1.1	900	3.8	416	4.0	167	60.0%	<4.0	3.8	
1.0	924	10.0	407	9.8	210	48.4%	<2.0	1.0–1.3	Reaction time/s
1.1	920	12.0	363	12.1	271	25.3%	<6.0	0.4–0.6	
1.3	918	8.0	424	9.3	174	59.0%	<3.0	75	Injection pressure/kPa
1.3	910	8.0	424	10.8	168	60.4%	<3.0	45	
0.6	914	9.0	531	9.3	445	16.2%	<3.0		NH ₃ ·H ₂ O concentration /vol.%
1.0	927	9.0	531	9.4	227	57.3%	<3.0	7.0	
1.6	924	9.0	531	8.7	178	66.5%	<5.0		

Table 3 also showed the effects of NSR on the NO_x reduction rate and ammonia slip by using 6.5 vol.% NH₃·H₂O as NO_x reducing agent. Combining with the previous analysis, it can be seen that NO_x reduction rate and ammonia slip had little change when the NH₃·H₂O concentration was 13 vol.% or 6.5 vol.% with the same other conditions, which indicated that the influence of NH₃·H₂O concentration on NO_x reduction was not the main factor. The pressure of NH₃·H₂O injection had little effect on the NO_x reduction and ammonia slip either. No significant changes in the NO_x reduction rate and ammonia slip have been found when the NH₃·H₂O injection pressure was 75 kPa or 45 kPa.

4. NO_x Emission Behavior and Prospects of Denitrification Technology

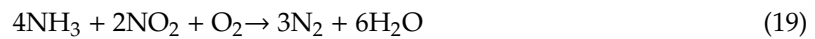
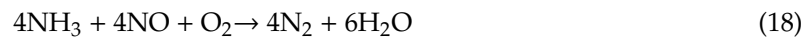
4.1. NO_x Emission Behavior

The grate-rotary kiln process consists of three parts: The grate, the rotary kiln, and the cooler [30]. Green pellets are dried and preheated through the four zones of the grate (i.e., updraft drying zone, downdraft drying zone, tempered preheating zone, and preheating zone), preheated pellets are then fed into the rotary kiln for roasting at a high temperature to obtain better metallurgy performance, and in the rotary kiln, most often coke oven gas is used as fuel to meet the requirement of high temperatures. The flame temperature of the burner in the rotary kiln can even reach 1600–1850 °C with the combustion of gas, a large amount of thermal NO_x generates for the temperature well above 1300 °C, and it dominates NO_x formation, accounting for more than 80%. The generated NO_x is firstly circulated with the hot flue gas to the preheating zone, and then to the downdraft drying zone. The terminal NO_x emission usually exceeds 200 mg/m³.

Although most NO_x generates in the rotary kiln, the temperature required by pellets roasting is too high for the effective application of low-NO_x control technologies. Compared with rotary kiln, the preheating zone has a more appropriate temperature distribution (900–1050 °C) to implement low-NO_x control technologies, such as selective non-catalytic reduction (SNCR). Furthermore, all NO_x generated in the rotary kiln enters into the preheating zone with the flue gas according to direction the of air flow in the grate-rotary kiln process, the NO_x content in the flue gas of preheating zone consequently reaches a relatively high level, exceeding 400 mg/m³. Moreover, there will be sufficient time for denitrification reaction in the preheating zone, since the length of it usually exceeds 10 m.

The application of advanced reburning in the preheating zone is considered one of the most direct and effective ways to reduce NO_x emission in grate-rotary kiln. An additional burner can be added to preheating zone, coal gas can be used as a reburning fuel when injected into the high NO_x flue gas, and this creates a reducing environment to effectively promote NO_x reduction and provide the temperature required for pellets preheating and advanced reburning as well. Ammonia is sprayed into the preheating zone, NO_x is reduced in the following four reactions [31,32]:





At the appropriate temperature (about 1000 °C) and in the temperature window range of 150 °C, a certain number of OH generates, promoting the transformation of NH₃ into NH₂ in large quantities, and the NH₂ is highly selective for NO_x reduction, which triggers the chain reaction. An advanced reburning denitrification device was installed to the grate-rotary kiln production line of an annual output of 1.2 million tons of pellets. The process flow was shown in Figure 4. It can be seen that the whole device was composed of ammonia storage and transportation system, ammonia water mixing system, ammonia water metering system, ammonia water spraying system, and wastewater discharge system.

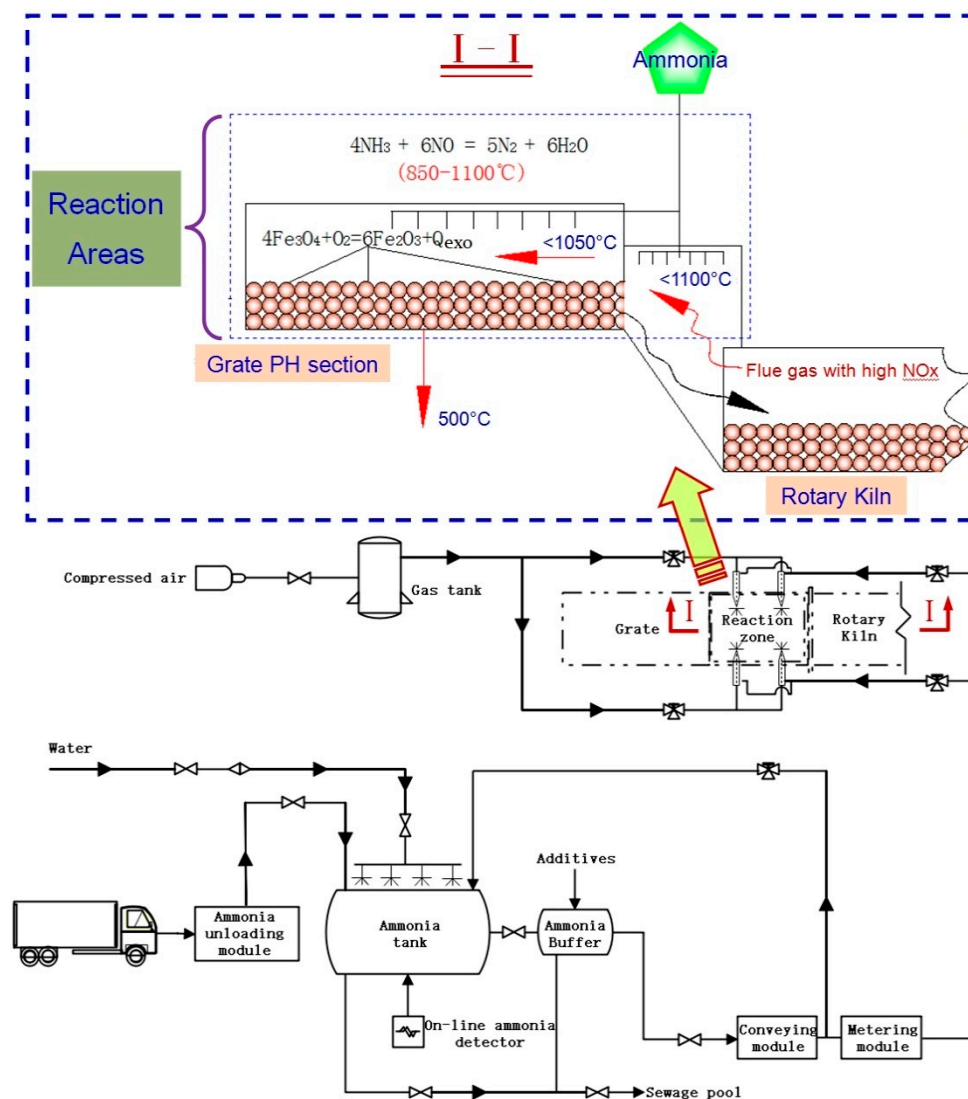


Figure 4. Process flow of advanced reburning denitrification device and its application.

Given the high temperature (850~1100 °C), high-concentrated NO_x (300~1000 mg/m³), wide reaction areas (the reaction time in the hood will more than 0.5 s) of the PH and transition section of the chain grate, An advanced reburning denitrification device can be added to the appropriate position of the chain grate PH section (In the blue box, as shown in Figure 4), which will be beneficial to lighten the burden of the NO_x terminal treatment and achieve ultra-low nitrogen oxide emissions. The denitration effects before and after applying advanced reburning were shown in Table 4. As shown

in Table 4, the emission concentration of NO_x was 275–296 mg/Nm^3 before applying advanced reburning in the pellet production process, and it reduced to 163–182 mg/Nm^3 after the adoption of this technology. The amount of flue gas was 396,000–410,000 Nm^3/h . The denitrification efficiency reached nearly 40%, and the escape concentration of ammonia was less than 10 ppm at the same time, which showed a remarkable denitrification effect.

Table 4. Denitrification effect of flue gas before and after advanced reburning.

Components	Kiln Tail Gas			System Exhaust Gas		
	NO_x $/\text{mg Nm}^{-3}$	$\text{O}_2/\%$	NO_x Annual Emissions/ t a^{-1}	NO_x $/\text{mg Nm}^{-3}$	$\text{O}_2/\%$	NH_3 $/\text{mg Nm}^{-3}$
Before process	680–810	15.4–17.2	≈939	275–296	17.3–18.1	-
After process	-	-	≈582	163–188	17.2–17.9	7.1–9.8

4.2. Prospects of Denitrification Technology

A series of denitrification measures, such as SCR and flue gas circulation, can be combined with advanced reburning technology in order to achieve ultra-low emission standard of NO_x in the oxidation pellet production of grate-rotary kiln process, as shown in Figure 5.

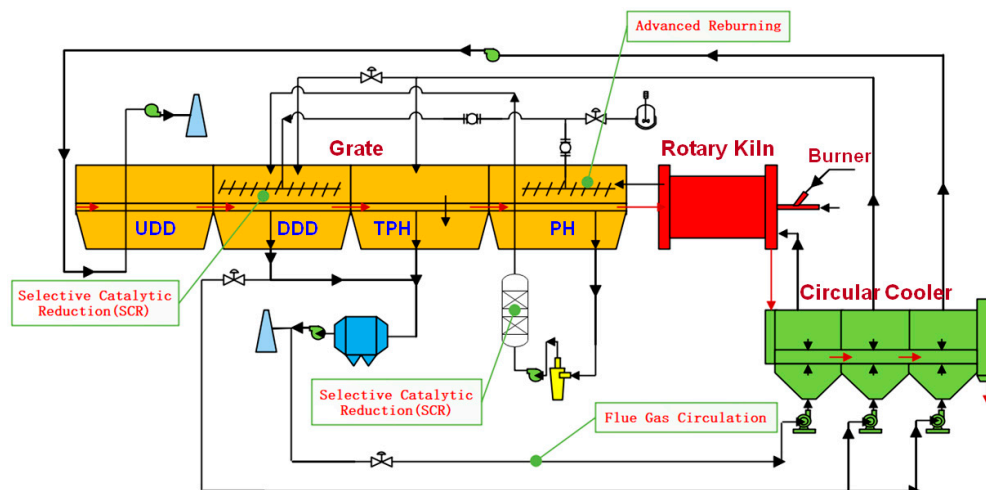


Figure 5. Denitrification mechanism of advanced reburning technology.

In detail, the flue gas discharged from the PH section can be denitrified by SCR after dust removal, SCR can also be applied to the end treatment of flue gas in the DDD section at the same time. In addition, the flue gas discharged from the DDD and TPH sections can be circulated to each section of the cooler as required. It avoids the problems of low denitrification efficiency and excess ammonia slip caused by the high concentration of NO_x in flue gas when SCR is used directly to denitrify flue gas, thus realizing the purpose of ultra-low NO_x emission in pellet production.

5. Conclusions

The influences of temperature, NSR, and other factors on NO_x reduction, as well as ammonia slip, was investigated; and optimum operating parameters of denitrification in the grate-rotary kiln process for pellet production was obtained. Temperature and NSR are the key factors affecting the NO_x reduction rate in advanced reburning. It is conducive to reducing NO_x when the temperature is 900 °C, NSR is 1.2, and reaction time is more than one second. Better denitrification effect can be obtained on flue gas with higher initial NO_x concentration under the preceding conditions, for flue gas with initial NO_x concentration of about 400 ppm, NO_x reduction rate can reach 55–65% with an ammonia slip concentration of 2 mg/m^3 , and NO_x reduction rate can be higher than 70% with an ammonia slip concentration of 3 mg/m^3 when initial NO_x concentration is around

680 ppm. Additionally, urea solution has the best denitrification effect, then $\text{NH}_3 \cdot \text{H}_2\text{O}$, and then NH_4HCO_3 solution. Moreover, regarding additives, the denitrification effect of the vanadium-titanium catalyst is better than that of ethanol and NaCl, while NaCl plays a promotive role at low NSR (1.0, for example). However, O_2 concentration, $\text{NH}_3 \cdot \text{H}_2\text{O}$ concentration, and injection pressure have little effect on reducing NO_x . A series of denitrification measures that include advanced reburning technology for achieving NO_x ultra-low emission in the oxidation pellet production can be implemented.

Author Contributions: Conceptualization, B.H. and P.H.; methodology, P.H.; investigation, B.L., Z.X. and L.L.; data curation, L.L. and G.C.; writing—original draft preparation, B.H. and B.L.; writing—review and editing, P.H., Z.X. and J.W.; project administration, P.H. All authors have read and agreed to the published version of the manuscript.

Funding: The authors acknowledge the support that provided by Hunan Provincial Natural Science Foundation of China (2019JJ51007), National Natural Science Foundation of China (51304149), Key Project of Scientific Research Plan of Hubei Provincial Department of Education (D20191106), National Training Program of Innovation and Entrepreneurship for Undergraduates (201810488021) and Key Research Project of Science and Technology Innovation Fund for College Students of WUST (17ZRB086).

Acknowledgments: Critical comments and thoughtful suggestions by anonymous reviewers are highly appreciated.

Conflicts of Interest: The authors declare no conflict of interest.

References

- Zhang, H.J.; She, X.F.; Han, Y.H.; Wang, J.S.; Zeng, F.B.; Xue, Q.G. Softening and Melting Behavior of Ferrous Burden under Simulated Oxygen Blast Furnace Condition. *J. Iron Steel Res. Int.* **2015**, *22*, 297–303. [\[CrossRef\]](#)
- Bolen, J. Modern air pollution control for iron ore induration. *Min. Metall. Explor.* **2014**, *31*, 103–114. [\[CrossRef\]](#)
- Zhang, F.; Zhu, D.; Pan, J.; Guo, Z.; Yang, C. Effect of basicity on the structure characteristics of chromium-nickel bearing iron ore pellets. *Powder Technol.* **2019**, *342*, 409–417. [\[CrossRef\]](#)
- Gan, M.; Ji, Z.; Fan, X.; Chen, X.; Zheng, R.; Gao, L.; Wang, G.; Jiang, T. Value-added utilization of waste silica powder into high-quality chromite pellets preparation process. *Powder Technol.* **2018**, *328*, 122–129. [\[CrossRef\]](#)
- Yi, L.; Huang, Z.; Jiang, T.; Zhong, R.; Liang, Z. Iron ore pellet disintegration mechanism in simulated shaft furnace conditions. *Powder Technol.* **2017**, *317*, 89–94. [\[CrossRef\]](#)
- Stjernberg, J.; Ion, J.C.; Antti, M.L.; Nordin, L.O.; Lindblom, B.; Odén, M. Extended studies of degradation mechanisms in the refractory lining of a rotary kiln for iron ore pellet production. *J. Eur. Ceram. Soc.* **2012**, *32*, 1519–1528. [\[CrossRef\]](#)
- Stjernberg, J.; Isaksson, O.; Ion, J.C. The grate-kiln induration machine: History, advantages, and drawbacks, and outline for the future. *J. S. Afr. Inst. Min. Metall.* **2015**, *115*, 137–144. [\[CrossRef\]](#)
- Sun, W.; Zhou, Y.; Lv, J.; Wu, J. Assessment of multi-air emissions: Case of particulate matter (dust), SO_2 , NO_x and CO_2 from iron and steel industry of China. *J. Clean. Prod.* **2019**, *232*, 350–358. [\[CrossRef\]](#)
- Lv, W.; Sun, Z.; Su, Z. Life cycle energy consumption and greenhouse gas emissions of iron pelletizing process in China, a case study. *J. Clean. Prod.* **2019**, *233*, 1314–1321. [\[CrossRef\]](#)
- Wang, X.; Lei, Y.; Yan, L.; Liu, T.; Zhang, Q.; He, K. A unit-based emission inventory of SO_2 , NO_x and PM for the Chinese iron and steel industry from 2010 to 2015. *Sci. Total Environ.* **2019**, *676*, 18–30. [\[CrossRef\]](#)
- Fan, X.H.; Yang, G.M.; Chen, X.L.; Gao, L.; Huang, X.X.; Li, X. Predictive models and operation guidance system for iron ore pellet induration in traveling grate–rotary kiln process. *Comput. Chem. Eng.* **2015**, *79*, 80–90. [\[CrossRef\]](#)
- Zhang, Q.; Zhao, X.; Lu, H.; Ni, T.; Li, Y. Waste energy recovery and energy efficiency improvement in China's iron and steel industry. *Appl. Energy* **2017**, *191*, 502–520. [\[CrossRef\]](#)
- Zhu, T.; Hu, Y.; Tang, C.; Wang, L.; Liu, X.; Deng, L.; Che, D. Experimental study on NO_x formation and burnout characteristics of pulverized coal in oxygen enriched and deep-staging combustion. *Fuel* **2020**, *272*, 117639. [\[CrossRef\]](#)
- Zhou, C.; Wang, Y.; Jin, Q.; Chen, Q.; Zhou, Y. Mechanism analysis on the pulverized coal combustion flame stability and NO_x emission in a swirl burner with deep air staging. *J. Energy Inst.* **2019**, *92*, 298–310. [\[CrossRef\]](#)

15. Edland, R.; Normann, F.; Fredriksson, C.; Andersson, K. Implications of fuel choice and burner settings for combustion efficiency and NO_x formation in PF-fired iron ore rotary kilns. *Energy Fuels* **2017**, *31*, 3253–3261. [[CrossRef](#)]
16. Zhou, H.; Huang, Y.; Mo, G.; Liao, Z.; Cen, K. Experimental investigations of the conversion of fuel-N, volatile-N and char-N to NO_x and N₂O during single coal particle fluidized bed combustion. *J. Energy Inst.* **2017**, *90*, 62–72. [[CrossRef](#)]
17. Edland, R.; Smith, N.; Allguren, T.; Fredriksson, C.; Normann, F.; Haycock, D.; Johnson, C.; Frandsen, J.; Fletcher, T.H.; Andersson, K. Evaluation of NO_x-Reduction Measures for Iron-Ore Rotary Kilns. *Energy Fuels* **2020**, *34*, 4934–4948. [[CrossRef](#)]
18. Li, J.; Chang, H.; Ma, L.; Hao, J.; Yang, R.T. Low-temperature selective catalytic reduction of NO_x with NH₃ over metal oxide and zeolite catalysts—A review. *Catal. Today* **2011**, *175*, 147–156. [[CrossRef](#)]
19. Fan, W.; Wu, X.; Guo, H.; Zhu, J.; Liu, P.; Chen, C.; Wang, Y. Experimental study on the impact of adding NH₃ on NO production in coal combustion and the effects of char, coal ash, and additives on NH₃ reducing NO under high temperature. *Energy* **2019**, *173*, 109–120. [[CrossRef](#)]
20. Fu, S.; Song, Q.; Yao, Q. Mechanism study on the adsorption and reactions of NH₃, NO, and O₂ on the CaO surface in the SNCR deNO_x process. *Chem. Eng. J.* **2016**, *285*, 137–143. [[CrossRef](#)]
21. Nguyen, T.D.; Lim, Y.I.; Kim, S.J.; Eom, W.H.; Yoo, K.S. Experiment and computational fluid dynamics (CFD) simulation of urea-based selective noncatalytic reduction (SNCR) in a pilot-scale flow reactor. *Energy Fuels* **2008**, *22*, 3864–3876. [[CrossRef](#)]
22. Liu, H.; Zhao, S.; You, C.; Wang, H. Experimental Study on the Enhancement of SNCR Denitrification Process with Methane and Propane in A Circulating Fluidized Bed. *Ind. Eng. Chem. Res.* **2019**, *58*, 7825–7833. [[CrossRef](#)]
23. Du, L.; Jin, B.; Zheng, X.; Niu, M. Effect of reburning zone conditions on no reduction efficiency in an online precalciner-type kiln system. *Environ. Prog. Sustain. Energy* **2016**, *35*, 439–446. [[CrossRef](#)]
24. Fan, W.; Zhu, T.; Sun, Y.; Lv, D. Effects of gas compositions on NO_x reduction by selective non-catalytic reduction with ammonia in a simulated cement precalciner atmosphere. *Chemosphere* **2014**, *113*, 182–187. [[CrossRef](#)]
25. Li, S.; Ge, Y.; Wei, X. Experiment on NO_x reduction by advanced reburning in cement precalciner. *Fuel* **2018**, *224*, 235–240. [[CrossRef](#)]
26. Zhuang, H.; Niu, Y.; Gong, Y.; Zhang, Y.; Zhang, Y.; Hui, S. Influence of Biomass Reburning on NO_x Reductions during Pulverized Coal Combustion. *Energy Fuels* **2017**, *31*, 5597–5602. [[CrossRef](#)]
27. Yamamoto, T.; Kajimura, S. Kinetic Study on NO Reduction Using Dimethyl Ether as a Reburning Fuel. *Energy Fuels* **2017**, *31*, 12500–12507. [[CrossRef](#)]
28. Kang, Z.; Yuan, Q.; Zhao, L.; Dai, Y.; Sun, B.; Wang, T. Study of the performance, simplification and characteristics of SNCR de-NO_x in large-scale cyclone separator. *Appl. Therm. Eng.* **2017**, *123*, 635–645. [[CrossRef](#)]
29. Fu, S.; Song, Q.; Yao, Q. Mechanism of the Reaction between HNCO and CaO in the Urea-Selective Non-catalytic Reduction deNO_x Process. *Energy Fuels* **2017**, *31*, 5318–5323. [[CrossRef](#)]
30. Forsmo, S.P.E.; Forsmo, S.E.; Samskog, P.O.; Björkman, B.M.T. Mechanisms in oxidation and sintering of magnetite iron ore green pellets. *Powder Technol.* **2008**, *183*, 247–259. [[CrossRef](#)]
31. Lyon, R.K. Thermal DeNO_x controlling nitrogen oxides emissions by a noncatalytic process. *Environ. Sci. Technol.* **1987**, *21*, 231–236. [[CrossRef](#)] [[PubMed](#)]
32. Lee, G.W.; Shon, B.H.; Yoo, J.G.; Jung, J.H.; Oh, K.J. The influence of mixing between NH₃ and NO for a De-NO_x reaction in the SNCR process. *J. Ind. Eng. Chem.* **2008**, *14*, 457–467. [[CrossRef](#)]

Publisher's Note: MDPI stays neutral with regard to jurisdictional claims in published maps and institutional affiliations.



© 2020 by the authors. Licensee MDPI, Basel, Switzerland. This article is an open access article distributed under the terms and conditions of the Creative Commons Attribution (CC BY) license (<http://creativecommons.org/licenses/by/4.0/>).